ACS OMEGA

Article

Cite This: ACS Omega 2018, 3, 17368−17375

http://pubs.acs.org/journal/acsodf

Identification of a Tool Compound to Study the Mechanisms of Functional Selectivity between D_2 and D_3 Dopamine Receptors

Irene Reyes-Resina,[†,‡,▽] Abdelouahid Samadi,[*,§,▽] Gemma Navarro,[†,∥,▽] Haythem A. Saadeh,[*,§,⊥] Mohammad A. Khasawneh,[§] Jordi Mestres,[#] José Marco-Contelles,[*,¶] and Rafael Franco[*,†,‡]

[†]Centro de Investigación en Red, Enfermedades Neurodegenerativas (CiberNed), Instituto de Salud Carlos III, Sinesio Delgado 6, 28029 Madrid, Spain

[‡]Department of Biochemistry and Molecular Biomedicine, School of Biology, Universitat de Barcelona, Diagonal 643, 08028 Barcelona, Barcelona, Spain

[§]Department of Chemistry, College of Science, United Arab Emirates University, 15551 Al Ain, UAE

[∥]Department of Biochemistry and Physiology, School of Pharmacy and Food Sciences, Universitat de Barcelona, Avda Juan XXIII, 27, 08028 Barcelona, Spain

[⊥]Department of Chemistry, Faculty of Science, The University of Jordan, 11942 Amman, Jordan

[#]Research Group on Systems Pharmacology, Research Program on Biomedical Informatics (GRIB), IMIM Hospital del Mar Medical Research Institute & University Pompeu Fabra, Parc de Recerca Biomèdica (PRBB), Doctor Aiguader 88, 08003 Barcelona, Spain

[¶]Laboratory of Medicinal Chemistry, Organic Chemistry Institute (IQOG), Centro Superior de Investigaciones Científicas (CSIC), Juan de la Cierva 3, 28006 Madrid, Spain

Supporting Information

ABSTRACT: The search for synthetic selective compounds for G-protein-coupled receptors has provided a myriad of molecules with high selectivity and therapeutic potential. In some cases, however, selectivity is difficult to obtain. For instance, the selectivity ratio is relatively low for compounds acting on D_2 and D_3 dopamine receptors, which are targets of neurodegenerative diseases such as Parkinson's and Huntington's. From a therapeutic point of view, it is of interest the relative recent discovery of biased agonism, which is characterized by different signaling pathways engaged by different compounds acting on a given receptor. The aim of this paper was to investigate whether new piribedil-derived compounds could display higher selectivity for D_2 or D_3 receptor and/or provide biased signaling. The results show that selectivity was not different, but that one of the molecules described here, 5-((4-(pyrimidin-2-yl)piperazin-1-yl)methyl)quinolin-8-ol (**10**), does engage Gi-mediated signaling via D_2 or D_3 receptors, whereas it does not activate the mitogen-activated-protein kinase pathway, which is usually activated by dopamine receptor agonists.

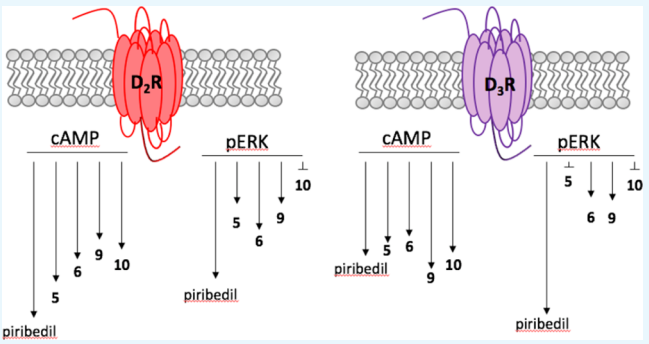

1. INTRODUCTION

Dopamine is one of the main neurotransmitters in the central nervous system (CNS), exerting its functions via five different receptors, D_1 to D_5, that are expressed in different neuronal types and in different regions of the brain. They all belong to the superfamily of G-protein-coupled receptors and are subdivided into D_1-like (D_1 and D_5), which are coupled to Gs and their activation leads to activation of adenylyl cyclase, and D_2-like (D_2, D_3 and D_4), which are coupled to Gi. Apart from mediating changes in one of the main intracellular second messengers, adenosine 3′:5′-cyclic phosphate (cAMP), they also engage the mitogen-activated-protein kinase (MAPK) pathway. Dopamine receptors are targets of a variety of neurological and neuropsychiatric diseases. First of all, agonists of dopamine receptors are used in Parkinson's disease (PD), which consists of denervation of striatal fibers projecting from the *substantia nigra*.[1] As an example, pramipexole is a non-ergot dopamine receptor agonist used in the therapy of PD and also of the restless legs syndrome.[2−4]

The piperazinyl pyrimidine (**I**, Figure 1) is a privileged motif present in a number of therapeutic agents showing anti-neuroinflammatory activity, such as compound **GIBH-130**, able to suppress the IL-1β in LPS-activated microglia, approved by China Food and Drug Administration for clinical

Received: September 25, 2018
Accepted: December 3, 2018
Published: December 14, 2018

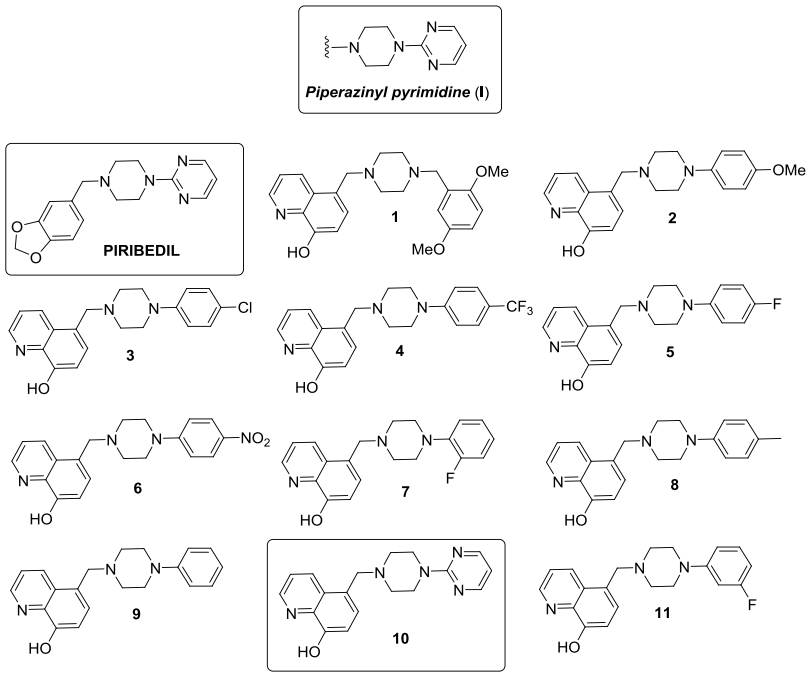

Figure 1. General structure of the *piperazinyl pyrimidine* motif (**I**), piribedil, and the 5-((arylpiperazin-1-yl)methyl)quinolin-8-ols **1**−**11**.

trials;[5] MW01-070C, a novel anti-neuroinflammatory agent;[6] Minozac, a drug under development as a water-soluble oral drug candidate for Alzheimer's disease;[7] MW01-5-188WH, a new molecule that selectively inhibits glial activation in the CNS,[8] or piribedil (Figure 1), an agent used for treating early and advanced PD that blocks α_2-adrenoreceptors with minor effects on serotoninergic, cholinergic, and histaminergic receptors.[9−11] Furthermore, and of interest for the present work, piribedil is a dopamine receptor agonist that also has potential in the therapy of PD.[12−14] However, piribedil taken by patients leads to side effects,[15] thus limiting its therapeutic potential. Piribedil is a mixed D_2/D_3 compound. It should be noted that D_3 compounds have potential to combat some of the side effects of dopamine-based therapies in PD, namely dyskinesia, which correlates with increases in the expression levels of the D_3 receptor.[16,17] Piribedil may therefore be a lead compound for development of D_3 receptor-selective compounds, as well as for gaining a better understanding of the function differences between D_2 and D_3 receptors.

With these ideas in mind, and continuing with our program on the synthesis and biological evaluation of *N*-arylpiperazine derivatives,[18,19] we have designed *N*-aryl analogues of piribedil, in which we have also substituted the 5-methylbenzo[*d*][1,3]-dioxole motif by the 5-methylquinolin-8-ol group, resulting in 5-((arylpiperazin-1-yl)methyl)quinolin-8-ol type of compounds **1**−**11** (Figure 1), incorporating a diverse array of electron-donating or electron-withdrawing substituents at different positions in the aryl ring. These modifications should have positive consequences because of the biological and physicochemical properties that the 8-hydroxyquinoline group underscored by drugs bearing this structural motif.[20,21] As a result from these studies, we have identified 5-((4-(pyrimidin-2-yl)piperazin-1-yl)methyl)quinolin-8-ol (**10**) (Figure 1) as a compound that exerts a profound bias in dopamine receptor signaling.

2. RESULTS AND DISCUSSION

2.1. Chemistry. The 5-((4-phenylpiperazin-1-yl)methyl)-8-hydroxyquinoline derivatives **1**, **2**, **3**,[22] **4**−**6**, **7**,[23] **8**, **9**,[23] **10**, and **11** were synthesized in a "one-pot reaction", by condensation of a solution of 5-(chloromethyl)-8-hydroxyquinoline hydrochloride[24] [or 2-(bromomethyl)-1,4-dimethoxybenzene[18] in the case of compound **1**] with the appropriate commercially available piperazine, in EtOH/tetrahydrofuran (THF) (1/1), during 15 min, at reflux. All compounds showed good analytical data in excellent agreement with their structure or the data described in the literature.

Inspection of the pharmacological data available for compounds **1**−**11** on public sources[25] revealed that, apart from piribedil, data are known only for 5-((4-phenylpiperazin-1-yl)methyl)quinolin-8-ol (**9**) (ChEMBL 1457644). Compound **9** was tested on a total of 52 assays for which IC_{50} and EC_{50} data were measured for 6 and 12 of them, respectively. Among them, of mention is the measured EC_{50} value of 3763 nM (pEC_{50} of 5.42) for streptokinase A. However, most surprisingly, even though molecule **9** shows close resemblance to piribedil and contains a phenyl piperazinyl moiety, a known privileged motif among dopamine active ligands, it was not tested on any G protein-couple receptor.

2.2. Biological Activity. The effect of the compounds synthesized on the D_2 and D_3 receptors was first tested in cAMP determination assays. As both D_2 and D_3 receptors are coupled to Gi, agonists lead to inhibition of the adenylyl cyclase. A total of 11 compounds at concentrations 200 nM and 1000 nM were tested in D_2- or D_3-receptor-expressing cells treated with forskolin, which leads to increases in cAMP. Any agonistic receptor-mediated effect will lead to a significant reduction in forskolin-induced cAMP levels. On the basis of this first (see Figure 2) screening, products 5, 6, 9, and 10 were selected for further studies. Dose-responses curves for cAMP and pERK1/2 assays are shown in Figure 3 in which it is shown that piribedil was the most potent compound. Raclopride, a nonselective D_2/D_3 receptor antagonist, was

DOI: 10.1021/acsomega.8b02509
ACS Omega 2018, 3, 17368−17375

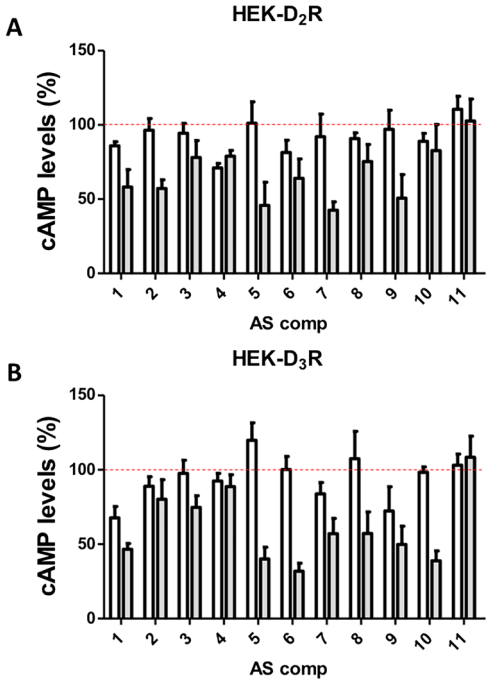

Figure 2. Signaling in HEK-293T cells expressing D_2R or D_3R. HEK-293T cells transfected with cDNA encoding for D_2R (A) or D_3R (B) were treated with compounds **1**−**11** (200 nM in white bars and 1000 nM in gray bars). cAMP accumulation was detected by time-resolved fluorescence energy transfer (TR-FRET) in the presence of 0.5 μM forskolin. cAMP production is expressed as % of levels obtained by using 0.5 μM forskolin. Data are mean ± standard error of the mean (SEM) of three different experiments in triplicates.

able to revert the effect of piribedil and piribedil-related compounds (Figure 4). Furthermore, non-transfected cells did not respond to the dopamine receptor agonists (Figure S1).

For those selected compounds and for piribedil, dose−response effects were measured (Figure 3). This approach was performed in cAMP determination and ERK1/2 phosphorylation assays in both D_2- and D_3-receptor-expressing cells. IC_{50} or EC_{50} values and the percentage of response were calculated using sumanirole (100 nM) as selective D_2-receptor or 7-OH-PIPAT (100 nM) as selective D_3-receptor agonists. The results are summarized in Table 1 which presents IC_{50} or EC_{50} values plus the percentage of effect respect to a reference compound. As shown in Figure 4, the effect of compounds on either D_2- or D_3-receptor-expressing cells was blocked by 1 μM raclopride, a potent nonselective D_2/D_3 receptor antagonist.

The results confirm that, in cAMP determination assays, piribedil is a preferential D_3 compound by 2 orders of magnitude.[11] However, a recent analysis of pharmacology data available for various compounds deposited in the ChEMBL database[25] revealed a fairly large data heterogeneity depending on the assay type and bioactivity endpoints.[26] Accordingly, we observed that piribedil selectivity for D_3 is lost when data on MAPK assays are considered. Interestingly, this loss of selectivity is very much in agreement with the known binding data available in public sources,[27] where the pK_i of piribedil for the D_2 and D_3 receptors is 6.85 and 6.60, respectively, albeit there is a difference of 3 orders of magnitude between binding pK_i data and our MAPK pEC_{50} data. In contrast, the results for the compounds synthesized in this work prove that none displayed a clearly marked selectivity for any of the two receptors. Remarkably, the potency of the majority of the compounds was fairly high. However, the most salient finding was the differential effect when, compound by compound, cAMP and MAPK results were compared. Apart from the disappearance of the selectivity mentioned above of piribedil when comparing the EC_{50} values in ERK1/2 phosphorylation assays, compound **10** showed a significant effect in cAMP assays but negligible capacity of activating the MAPK pathway.

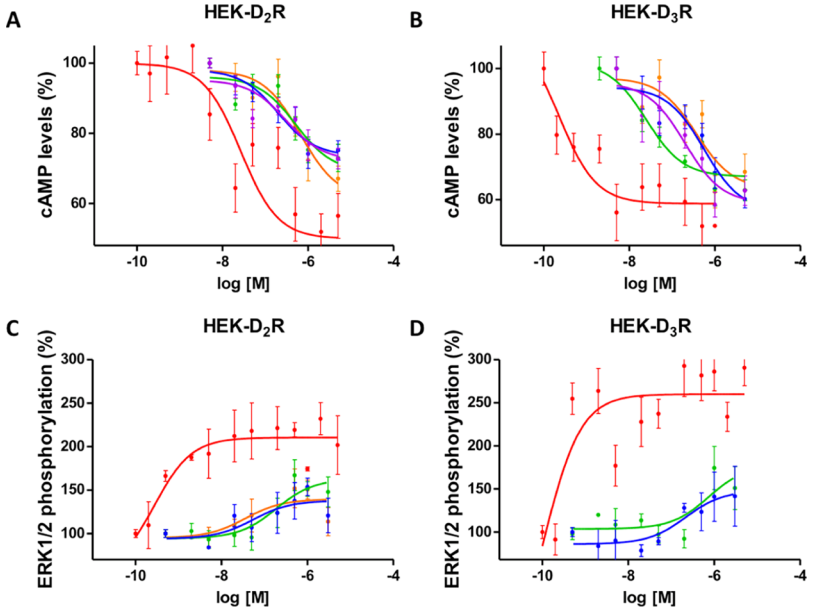

Figure 3. Dose response curves in HEK-293T cells expressing D_2R or D_3R. HEK-293T cells transfected with cDNA encoding for D_2R (A) or D_3R (B) were treated with piribedil (red) or compounds **5** (orange), **6** (green), **9** (blue), or **10** (purple). cAMP accumulation was detected by TR-FRET in the presence of 0.5 μM forskolin. cAMP production is expressed as percentage of levels obtained by using 0.5 μM forskolin. pERK1/2 phosphorylation is expressed as percentage over basal levels (100%). See General Methods for experimental details. Data are the mean ± SEM of five different experiments in triplicates. The concentration range was 0.2−5000 nM for piribedil and 2−3000 nM for the rest of compounds.

DOI: 10.1021/acsomega.8b02509
ACS Omega 2018, 3, 17368−17375

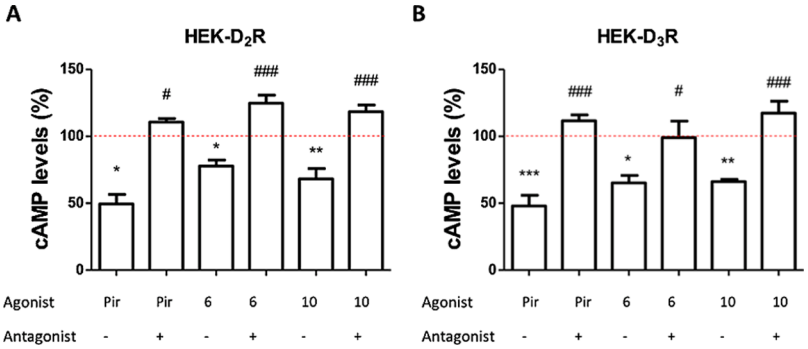

Figure 4. Reversion of agonist effect by raclopride in HEK-293T cells expressing D_2R or D_3R. HEK-293T cells transfected with cDNA encoding for D_2R (A, C) or D_3R (B, D) were pretreated with a dopamine receptor antagonist (1 μM raclopride) and subsequently treated with piribedil or compounds **6** and **10** (300 nM). cAMP accumulation was detected by TR-FRET in the presence of 0.5 μM forskolin. cAMP production is expressed as % of levels obtained by using 0.5 μM forskolin. Data are the mean ± SEM of three different experiments in triplicates. One-way ANOVA followed by Bonferroni's multiple comparison post-hoc test were used for statistical analysis. ($^{*}p < 0.05$, $^{**}p < 0.01$, $^{***}p < 0.001$; vs treatment with forskolin); ($^{\#}p < 0.05$, $^{\#\#\#}p < 0.001$; vs treatment with agonist).

Table 1. IC_{50} (cAMP Assays), EC_{50} (pERK1/2 MAPK Assays), and Percentage Values Versus Effect of 100 nM Sumanirole (D_2R) or 100 nM 7-OH-PIPAT (D_3R) of Piribedil and Compounds 5, 6, 9, and 10[a]

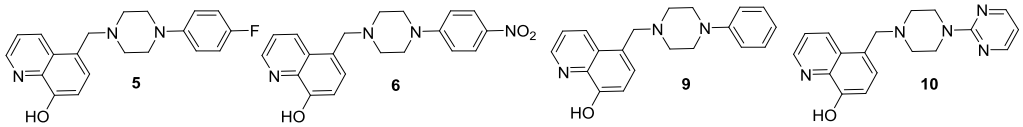

	HEK-D_2R reference: 100 nM sumanirole		HEK-D_3R reference: 100 nM 7-OH-PIPAT	
compound	cAMP pIC50 ± SD	MAPK pEC50 ± SD	cAMP pIC50 ± SD	MAPK pEC50 ± SD
piribedil	7.5 ± 0.5	9.5 ± 0.4	9.6 ± 0.6	9.5 ± 0.9
	167%	131%	118%	179%
5	6.1 ± 0.4	7.4 ± 0.9	6.4 ± 0.7	no effect
	129%	47%	105%	
6	6.2 ± 0.5	6.7 ± 0.4	7.7 ± 0.5	6.3 ± 1.3
	103%	75%	94%	50%
9	6.7 ± 0.4	7.3 ± 0.7	6.2 ± 0.4	6.6 ± 0.4
	88%	45%	125%	54%
10	6.5 ± 0.6	no significant effect	6.7 ± 0.5	no significant effect
	93%		118%	

[a]Percentages respect the effect of D_2 or D_3 receptor reference compounds were calculated using the maximal effect obtained after data fitting. Compounds **5** and **10** did not led to any significant ERK1/2 phosphorylation.

Therefore, molecule **10** disclosed a biased signaling in both D_2 and D_3 receptors.

This is important, as novel drug discovery approaches include allosteric modulators and biased agonists.

3. CONCLUSIONS

To sum up, in this report, we have described the design, synthesis, and biological evaluation on D_2 or D_3 receptors of new piribedil derivatives. Our results show that the synthesized compounds bind to the orthosteric center and not to any allosteric site. Remarkably, molecule **10** shows a marked biased agonism in both D_2 and D_3 receptors. Whereas variation in intracellular cAMP levels is surely due to engagement of Gi, ERK phosphorylation likely results from G-protein-independent signaling. Activation of G proteins involves large-scale movements of the α-helical domain of the α-subunit of the heterotrimeric G protein; the movement is necessary for GDP dissociation.[28−31] This mechanism of G protein activation occurs for products **5**, **6**, **9**, and **10** when they bind to and activate D_2R or D_3R (Table 1). The marked bias of piperazine **10** with absolute lack of action on the MAPK pathway is a most interesting, but unexpected result. Therefore, agent **10** can be considered a new tool compound to study the mechanisms of functional selectivity between D_2 and D_3 dopamine receptors, which are still poorly understood.

4. EXPERIMENTAL SECTION

4.1. Chemistry. Synthesis of Compounds 1−11.

4.1.1. General Methods. Melting points were determined in a Koffler apparatus and are uncorrected. ^{1}H NMR and ^{13}C NMR spectra were recorded at room temperature in $CDCl_3$ or DMSO-d_6 at 400 MHz and at 100.6 MHz, respectively, using solvent peaks [$CDCl_3$: 7.26 (D), 77.2 (C) ppm and DMSO-d_6 2.50 (D) and 39.7 (C) ppm] as internal references. The assignment of chemical shifts is based on standard NMR experiments (^{1}H, ^{13}C, ^{1}H−^{1}H COSY, ^{1}H−^{13}C HSQC, HMBC). Mass spectra were recorded on a gas chromatography/mass spectrometry (MS) spectrometer with an API-ES ionization source. Elemental analyses were performed at the IQOG (CSIC, Spain). Thin-layer chromatography analyses

DOI: 10.1021/acsomega.8b02509
ACS Omega 2018, 3, 17368−17375

were performed on silica F254 and detection by UV light at 254 nm. Column chromatography was performed on silica gel 60 (230 mesh) (Scheme 1).

Scheme 1. Synthesis of 5-((Arylpiperazin-1-yl)methyl)quinolin-8-ol Derivatives 1−9 and 11

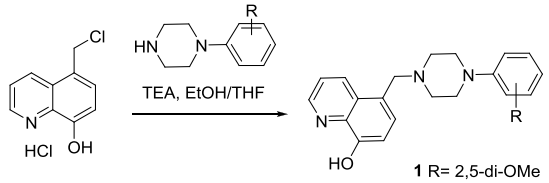

1 R= 2,5-di-OMe
2 R= 4-OMe
3 R= 4-Cl
4 R= 4-CF_3
5 R= 4-F
6 R= 4-NO_2
7 R= 2-F
8 R= 4-Me
9 R= H
11 R= 3-F

4.1.2. Synthesis of 5-((Arylpiperazin-1-yl)methyl)quinolin-8-ol Derivatives. To a solution of 1-arylpiperazine derivatives (0.1 mmol) in EtOH/THF (5/5 mL, v/v), TEA (three drops) and 5-(chloromethyl)quinolin-8-ol hydrochloride[30] (0.1 mmol) were added. The reaction was refluxed for the indicated time in each case. The solvent was evaporated, and the crude was diluted with CH_2Cl_2, washed with water, and extracted with CH_2Cl_2. The organic layer was dried with sodium sulfate and concentrated. Recrystallization in ethanol afforded the corresponding products as pure white solids (Scheme 2).

Scheme 2. Synthesis of 1-(2,5-Dimethoxybenzyl)piperazine

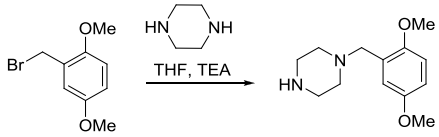

4.1.3. 1-(2,5-Dimethoxybenzyl)piperazine.[32] To a solution of piperazine (0.516 g, 6 mmol) in dry THF (5 mL), a solution of 2-(bromomethyl)-1,4-dimethoxybenzene[18] (0.231 g, 1 mmol) in THF (2 mL) was added dropwise. The reaction was refluxed for 30 min. Then, the reaction was diluted with EtOAc, washed with water, and extracted with EtOAc. The organic layer was dried with sodium sulfate, and the solvent was evaporated to afford a white solid 1-(2,5-dimethoxybenzyl)piperazine[22] (0.242 g, 99%); Rf = 0.1 (hexane/EtOAct, 1/1, v/v); IR (KBr) ν: 3002, 2948, 2832, 1497 cm^{-1}; ^1H NMR (400 MHz, $CDCl_3$): δ 6.97 (dd, J = 3.0, 0.4 Hz, 1H), 6.77 (s, 1H), 6.74 (d, J = 3.0 Hz, 1H), 3.76 (s, 3H, OMe), 3.76 (s, 3H, OMe), 3.51 (s, 2H, CH_2), 2.89 (t, J = 4.9 Hz, 4H, 2× CH_2), 2.47 (s, 4H, 2CH_2), 2.24 (s, 1H, NH); ^{13}C NMR (101 MHz, $CDCl_3$): δ 153.4, 152.0, 127.3, 116.3, 112.0, 111.5, 56.5, 56.1, 55.6, 54.2, 46.0; MS (EI$^+$, m/z): 236.3 $[M]^+$, 194.02, 151.1.

*4.1.4. 5-((4-(2,5-Dimethoxybenzyl)piperazin-1-yl)methyl)-quinolin-8-ol (**1**).* (0.217 g, 67%); Rf = 0.3 (dichloromethane/methanol, 10/1); mp 145−6 °C; IR (KBr) ν: 3331, 3021, 2798, 2657, 1580, 1511 cm^{-1}; ^1H NMR (400 MHz, $CDCl_3$): δ 8.75 (dd, J = 4.2, 1.6 Hz, 1H), 8.65 (dd, J = 8.5, 1.6 Hz, 1H), 7.43 (dd, J = 8.5, 4.2 Hz, 1H), 7.31 (d, J = 7.7 Hz, 1H), 7.05 (d, J = 7.7 Hz, 1H), 6.95 (d, J = 2.9 Hz, 1H), 6.73 (dt, J = 8.8, 5.9 Hz, 2H), 3.77 (s, 2H), 3.75 (s, 3H), 3.73 (s, 3H), 3.52 (s, 2H), 2.48 (s, 7H); ^{13}C NMR (101 MHz, $CDCl_3$): δ 153.3, 151.9, 151.6, 147.4, 138.5, 134.1, 128.7, 127.8, 127.4, 124.7, 121.3, 116.3, 112.0, 111.4, 108.5, 60.5, 56.0, 55.8, 55.6, 53.1, 53.0; MS (ESI$^+$, m/z): 394.2 $[M + H]^+$. Anal. Calcd for $C_{23}H_{27}N_3O_3$: C, 70.21; H, 6.92; N, 10.68. Found: C, 70.44; H, 7.01; N, 10.77.

*4.1.5. 5-((4-(4-Methoxyphenyl)piperazin-1-yl)methyl)-quinolin-8-ol (**2**).* (Reaction time: 15 min; 0.320 g, 92%); Rf = 0.5 (dichloromethane/methanol, 10/1); IR (KBr) ν: 3315, 2935, 2817, 2763, 1875, 1581, 1509, 1484 cm^{-1}; mp 173−4 °C; ^1H NMR (400 MHz, $CDCl_3$): δ 8.77 (dd, J = 4.2, 1.5 Hz, 1H), 8.69 (dd, J = 8.5, 1.5 Hz, 1H), 7.45 (dd, J = 8.5, 4.2 Hz, 1H), 7.35 (d, J = 7.7 Hz, 1H), 7.08 (d, J = 7.7 Hz, 1H), 6.90−6.77 (m, 4H), 3.84 (s, 2H, CH_2), 3.74 (s, 3H, OCH_3), 3.07−3.00 (m, 4H, 2× CH_2, piperazine), 2.67−2.57 (m, 4H, 2× CH_2, piperazine); ^{13}C NMR (101 MHz, $CDCl_3$): δ 148.9, 147.0, 142.8, 140.9, 133.9, 129.4, 124.2, 123.1, 119.7, 116.6, 113.3, 109.5, 103.9, 55.9 (CH_2), 50.7 (OCH_3), 48.4 (2× CH_2, piperazine), 45.9 (2× CH_2, piperazine); MS (ESI$^+$, m/z): 350.19 $[M + H]^+$. Anal. Calcd for $C_{21}H_{23}N_3O_2$: C, 72.18; H, 6.63; N, 12.03. Found: C, 72.01; H, 6.53; N, 11.89.

*4.1.6. 5-((4-(4-Chlorophenyl)piperazin-1-yl)methyl)-quinolin-8-ol (**3**).*[22] (Reaction time: 15 min; 0.340 g, 96%); Rf = 0.7 (dichloromethane/methanol, 10/1); mp 191−2 °C; IR (KBr) ν: 3304, 2825, 2773, 1865, 1596, 1579, 1498, 1480 cm^{-1}; ^1H NMR (400 MHz, $CDCl_3$): δ 8.77 (dd, J = 4.2, 1.5 Hz, 1H), 8.68 (dd, J = 8.5, 1.6 Hz, 1H), 7.45 (dd, J = 8.6, 4.2 Hz, 1H), 7.35 (d, J = 7.7 Hz, 1H), 7.19−7.12 (m, 2H), 7.07 (d, J = 7.7 Hz, 1H), 6.88−6.75 (m, 2H), 3.84 (s, 2H, CH_2), 3.20−3.01 (m, 4H, 2× CH_2, piperazine), 2.70−2.50 (m, 4H, 2× CH_2, piperazine); ^{13}C NMR (101 MHz, $CDCl_3$): δ 151.8, 149.9, 147.5, 138.6, 134.1, 129.0, 128.8, 127.8, 124.3, 124.2, 121.4, 117.1, 108.6, 60.6 (CH_2), 52.8 (2× CH_2, piperazine), 49.1 (2× CH_2, piperazine); MS (ESI$^+$, m/z): 354.13 $[M + H]^+$, 197.08, 158.07. Anal. Calcd for $C_{20}H_{20}ClN_3O$: C, 67.89; H, 5.70; N, 11.88. Found: C, 67.72; H, 5.88; N, 12.01.

*4.1.7. 5-((4-(4-(Trifluoromethyl)phenyl)piperazin-1-yl)-methyl)quinolin-8-ol (2i = **4**).* (Reaction time: 15 min; 0.363 g, 94%); Rf = 0.6 (dichloromethane/methanol, 10/1); mp 163−4 °C; IR (KBr) ν: 3317, 2820, 2771, 1897, 1616, 1578, 1508 cm^{-1}; ^1H NMR (400 MHz, $CDCl_3$): δ 8.79 (dd, J = 4.2, 1.6 Hz, 1H), 8.70 (dd, J = 8.6, 1.6 Hz, 1H), 7.50−7.43 (m, 3H), 7.36 (d, J = 7.7 Hz, 1H), 7.10 (d, J = 7.7 Hz, 1H), 6.89 (d, J = 8.7 Hz, 2H), 3.86 (s, 2H), 3.30−3.14 (m, 4H), 2.65−2.56 (m, 4H); ^{13}C NMR (101 MHz, $CDCl_3$): δ 153.2, 151.9, 147.6, 138.7, 134.1, 129.1, 127.8, 126.4, 126.3, 126.3, 126.3, 126.1, 124.1, 123.4, 121.5, 120.5, 120.1, 114.4, 108.6, 60.7 (CH_2), 52.7(2× CH_2, piperazine), 48.0 (2× CH_2, piperazine); MS (ESI$^+$, m/z): 387.89 $[M + H]^+$, 231.16, 157.82. Anal. Calcd for $C_{21}H_{20}F_3N_3O$: C, 65.11; H, 5.20; N, 10.85. Found: C, 65.32; H, 5.09; N, 10.77.

*4.1.8. 5-((4-(4-Fluorophenyl)piperazin-1-yl)methyl)-quinolin-8-ol (**5**).* (Reaction time: 15 min; 0.302 g, 82%); Rf = 0.8 (dichloromethane/methanol, 10/1); mp 175−7 °C; IR (KBr) ν: 3297, 2938, 2821, 1869, 1580, 1505, 1477 cm^{-1}; ^1H NMR (400 MHz, $CDCl_3$): δ 8.79 (d, J = 3.5 Hz, 1H), 8.70 (d, J = 8.5 Hz, 1H), 7.47 (dd, J = 8.5, 4.1 Hz, 1H), 7.36 (d, J = 7.7 Hz, 1H), 7.09 (d, J = 7.7 Hz, 1H), 6.94 (dd, J = 11.9, 5.3 Hz, 2H), 6.89−6.79 (m, 2H), 3.86 (s, 2H), 3.13−3.02 (m, 4H), 2.68−2.55 (m, 4H); ^{13}C NMR (101 MHz, $CDCl_3$); δ 158.2, 155.9, 151.9, 148.0, 148.0, 147.6, 138.7, 134.1, 129.0, 127.9,

DOI: 10.1021/acsomega.8b02509
ACS Omega 2018, 3, 17368−17375

124.3, 121.4, 117.7, 117.7, 115.5, 115.3, 108.6, 60.6 (CH_2), 53.0 (2× CH_2, piperazine), 50.18 (2× CH_2, piperazine); MS (ESI^+, m/z): 338.21 $[M + H]^+$, 180.95, 158.06. Anal. Calcd for $C_{20}H_{20}FN_3O$: C, 71.20; H, 5.98; N, 12.45. Found: C, 71.33; H, 5.77; N, 12.26.

*4.1.9. 5-((4-(4-Nitrophenyl)piperazin-1-yl)methyl)-quinolin-8-ol (**6**).* (Reaction time: 30 min; 0.320 g, 88%); Rf = 0.6 (dichloromethane/methanol, 10/1); mp 194−5 °C; IR (KBr) ν: 3392, 3006, 2934, 2833, 1837, 1587, 1503, 1459 cm^{-1}; ^1H NMR (400 MHz, $CDCl_3$): δ 8.78 (d, J = 4.1 Hz, 1H), 8.68−8.63 (m, 1H), 8.12−8.06 (m, 2H), 7.46 (dd, J = 8.5, 4.2 Hz, 1H), 7.34 (d, J = 7.7 Hz, 1H), 7.08 (d, J = 7.7 Hz, 1H), 6.78 (t, J = 6.4 Hz, 2H), 3.85 (s, 2H, CH_2), 3.40−3.32 (m, 4H, 2× CH_2, piperazine), 2.63−2.55 (m, 4H, 2× CH_2, piperazine); ^{13}C NMR (101 MHz, $CDCl_3$): δ 154.8, 152.0, 147.6, 138.6, 138.2, 134.0, 129.1, 127.8, 125.9, 123.8, 121.5, 112.5, 108.6, 60.5 (CH_2), 52.4 (2× CH_2, piperazine), 47.0 (2× CH_2, piperazine); MS (ESI^+, m/z): 365.14 $[M + H]^+$, 158.07. Anal. Calcd for $C_{20}H_{20}N_4O_3$: C, 65.92; H, 5.53; N, 15.38. Found: C, 65.71; H, 5.67; N, 15.44.

*4.1.10. 5-((4-(2-Fluorophenyl)piperazin-1-yl)methyl)-quinolin-8-ol (**7**).*[23] (Reaction time: 15 min; 0.330 g, 98%); Rf = 0.6 (dichloromethane/methanol, 10/1); mp 186−8 °C; IR (KBr) ν: 3307, 2935, 2812, 1863, 1610, 1578, 1505, 1477 cm^{-1}; ^1H NMR (400 MHz, $CDCl_3$): δ 8.78 (dd, J = 4.2, 1.5 Hz, 1H), 8.75−8.60 (m, 1H), 7.46 (dd, J = 8.5, 4.2 Hz, 1H), 7.36 (d, J = 7.7 Hz, 1H), 7.08 (d, J = 7.7 Hz, 1H), 7.05−6.99 (m, 2H), 6.98−6.86 (m, 2H), 3.86 (s, 2H), 3.04 (d, J = 4.2 Hz, 4H), 2.70−2.58 (m, 4H); ^{13}C NMR (101 MHz, $CDCl_3$): δ 156.9, 154.4, 151.8, 147.5, 140.1, 140.1, 138.6, 134.1, 129.0, 127.9, 124.4, 124.4, 124.3, 122.3, 122.2, 121.34, 118.8, 118.8, 116.1, 115.9, 108.7, 60.6 (CH_2), 53.1 (2× CH_2, piperazine), 50.5 (CH_2, piperazine), 50.5 (CH_2, piperazine); MS (ESI^+, m/z): 338.21 $[M + H]^+$, 181.01, 158.13. Anal. Calcd for $C_{20}H_{20}FN_3O$: C, 71.20; H, 5.98; N, 12.45. Found: C, 71.09; H, 5.71; N, 12.63.

*4.1.11. 5-((4-(p-Tolyl)piperazin-1-yl)methyl)quinolin-8-ol (**8**).* (Reaction time: 15 min; 0.369 g, 98%); Rf = 0.5 (dichloromethane/methanol, 10/1); mp 167−8 °C; IR (KBr) ν: 3313, 2820, 2762, 1611, 1581, 1509, 1483 cm^{-1}; ^1H NMR (400 MHz, $CDCl_3$): δ 8.78 (dd, J = 4.2, 1.5 Hz, 1H, CH-2), 8.71 (dd, J = 8.6, 1.5 Hz, 1H, CH-4), 7.47 (dd, J = 8.6, 4.2 Hz, 1H, CH-3), 7.37 (d, J = 7.7 Hz, 1H), 7.07 (dd, J = 14.0, 8.1 Hz, 3H), 6.82 (d, J = 8.6 Hz, 2H), 3.86 (s, 2H, CH_2), 3.17−2.96 (m, 4H, 2× CH_2, piperazine), 2.70−2.56 (m, 4H, 2× CH_2, piperazine), 2.26 (s, 3H, CH_3); ^{13}C NMR (101 MHz, $CDCl_3$): δ 151.8, 149.2, 147.6, 138.7, 134.1, 129.6, 129.1, 129.0, 127.9, 121.5, 116.4, 108.6, 60.7(CH_2), 53.1 (2× CH_2, piperazine), 49.7 (2× CH_2, piperazine), 20.4 (CH_3); MS (ESI^+, m/z): 334.24 $[M + H]^+$, 177.17, 158.17. Anal. Calcd for $C_{21}H_{23}N_3O$: C, 75.65; H, 6.95; N, 12.60. Found: C, 75.82; H, 6.75; N, 12.39.

*4.1.12. 5-((4-Phenylpiperazin-1-yl)methyl)quinolin-8-ol (**9**).*[23] (Reaction time: 25 min; 0.430 g, 98%); Rf = 0.8 (dichloromethane/methanol, 10/1); mp 189−190 °C; IR (KBr) ν: 3312, 2816, 1599, 1578, 1505, 1493, 1478 cm^{-1}; ^1H NMR (400 MHz, $CDCl_3$): δ 8.80 (d, J = 4.2 Hz, 1H, CH-2), 8.72 (dd, J = 8.6, 1.3 Hz, 1H, CH-4), 7.48 (ddd, J = 8.5, 4.2, 0.6 Hz, 1H, CH-3), 7.38 (d, J = 7.7 Hz, 1H), 7.30−7.21 (m, 1H), 7.10 (d, J = 7.7 Hz, 1H), 6.92 (d, J = 8.5 Hz, 1H), 6.85 (td, J = 7.7, 0.6 Hz, 1H), 3.87 (s, 2H, CH_2), 3.20−3.13 (m, 4H, 2CH_2, piperazine), 2.69−2.59 (m, 4H, 2CH_2, piperazine); ^{13}C NMR (101 MHz, $CDCl_3$): δ 147.0, 146.5, 142.8, 133.9, 129.4, 124.3, 124.2, 123.1, 119.6, 116.6, 114.8, 111.2, 103.8, 55.9 (CH_2), 48.2 (2× CH_2, piperazine), 44.4 (2× CH_2, piperazine); MS (ESI^+, m/z): 320.19 $[M + H]^+$, 161.08, 157.76. Anal. Calcd for $C_{20}H_{21}N_3O$: C, 75.21; H, 6.63; N, 13.16. Found: C, 75.42; H, 6.83; N, 13.09.

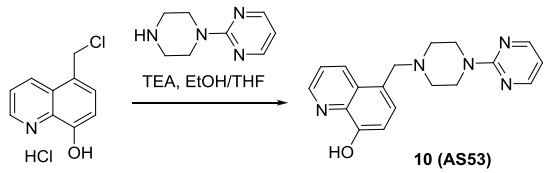

*4.1.13. 5-((4-(Pyrimidin-2-yl)piperazin-1-yl)methyl)-quinolin-8-ol (**10**).* Prepared form 5-(chloromethyl)quinolin-8-ol hydrogen chloride,[24] and 2-(piperazin-1-yl)pyrimidine (reaction time: 30 min; 0.307 g, 96%); Rf = 0.7 (dichloromethane/methanol, 10/1); mp 143−5 °C; IR (KBr) ν: 3342, 2811, 1593, 1542, 1500, 1475 cm^{-1}; ^1H NMR (400 MHz, DMSO-d_6): δ 8.78 (dd, J = 4.2, 1.5 Hz, 1H), 8.70 (dd, J = 8.5, 1.5 Hz, 1H), 8.27 (dd, J = 4.7, 0.6 Hz, 2H), 7.46 (dd, J = 8.5, 4.2 Hz, 1H), 7.33 (d, J = 7.7 Hz, 1H), 7.07 (d, J = 7.7 Hz, 1H), 6.45 (t, J = 4.7 Hz, 1H), 3.81 (s, 2H, CH_2), 3.78−3.73 (m, 4H, 2× CH_2, piperazine), 2.56−2.43 (m, 4H, 2× CH_2, piperazine); ^{13}C NMR (101 MHz, DMSO-d_6): δ 161.5, 157.7, 151.8, 147.5, 138.7, 134.1, 129.0, 127.9, 124.3, 121.5, 109.7, 108.6, 60.8 (CH_2), 52.9 (2× CH_2, piperazine), 43.7 (2× CH_2, piperazine); MS (ESI^+, m/z): 322.14 $[M + H]^+$, 1665.19, 158.16. Anal. Calcd for $C_{18}H_{19}N_5O$: C, 67.27; H, 5.96; N, 21.79. Found: C, 67.41; H, 6.11; N, 21.64.

*4.1.14. 5-((4-(3-Fluorophenyl)piperazin-1-yl)methyl)-quinolin-8-ol (**11**).* (Reaction time: 15 min; 0.279 g, 83%); Rf = 0.7 (hexane/EtOAct, 1/1); mp 162−3 °C; IR (KBr) ν: 3312, 2936, 2820, 1612, 1579, 1506 cm^{-1}; ^1H NMR (400 MHz, $CDCl_3$): δ 8.79 (dd, J = 4.2, 1.5 Hz, 1H), 8.70 (dd, J = 8.5, 1.5 Hz, 1H), 7.47 (dd, J = 8.5, 4.2 Hz, 1H), 7.36 (d, J = 7.7 Hz, 1H), 7.16 (dd, J = 15.3, 8.2 Hz, 1H), 7.09 (d, J = 7.7 Hz, 1H), 6.64 (dd, J = 8.4, 2.3 Hz, 1H), 6.53 (ddt, J = 15.3, 8.2, 2.4 Hz, 2H), 3.85 (s, 2H), 3.20−3.11 (m, 4H), 2.67−2.53 (m, 4H); ^{13}C NMR (101 MHz, $CDCl_3$): δ 165.0, 162.6, 153.0, 152.9, 151.9, 147.6, 138.7, 134.1, 130.1, 130.0, 129.0, 127.9, 124.2, 121.5, 111.1, 111.0, 108.6, 105.8, 105.6, 102.7, 102.4, 60.6 (CH_2), 52.8 (2× CH_2, piperazine), 48.6 (2× CH_2, piperazine); MS (ESI^+, m/z): 338.27 $[M + H]^+$, 181.08, 158.06. Anal. Calcd for $C_{20}H_{20}FN_3O$: C, 71.20; H, 5.98; N, 12.45. Found: C, 71.36; H, 6.02; N, 12.02.

4.2. Biological Evaluation. *4.2.1. Cell Culture and Transfection.* Human embryonic kidney 293T (HEK-293T) cells were grown in Dulbecco's modified Eagle's medium supplemented with 2 mM L-glutamine, 1 mM sodium pyruvate, 100 units/mL penicillin/streptomycin, and 5% (v/v) fetal bovine serum [all supplements were from Invitrogen, (Paisley, Scotland, UK)]. Cells were maintained at 37 °C in a humidified atmosphere of 5% CO_2 and were passaged, with trypsin (Thermo Fisher Scientific, Waltham, MA, USA), when they were 80−90% confluent, that is, approximately twice a week. Cells were transiently transfected with the polyethylenimine (Sigma, St. Louis, MO, USA) method as previously described.[31,32] Experiments were carried out in cells expressing dopamine D_2 or D_3 receptors.

4.2.2. cAMP Determination and ERK Phosphorylation Assays. Details of the protocols are provided elsewhere.[33,34] For cAMP assays, cells were serum deprived and a phosphodiesterases inhibitor was used (50 μM zardaverine).

DOI: 10.1021/acsomega.8b02509
ACS Omega 2018, 3, 17368−17375

Agonists were added 15 min before addition of forskolin (0.5 μM) forskolin, and reaction took place for 60 min (25 °C). The cAMP level was determined using the Lance Ultra cAMP kit (PerkinElmer, Waltham, MA, USA), and readings were performed in a PHERAstar (BMG Lab technologies, Offenburg, GE) equipped with an HTRF optical module. For pERK1/2 determination, the procedure was similar, but cells were washed prior use of lysing buffer (20 min 0°−4°). Supernantants (10 μL) were analyzed using ad hoc AlphaScreen SureFire and the EnSpire Reader (both from PerkinElmer, Waltham, MA, USA). When indicated, the antagonist was added 15 min prior to the addition of the agonist. The lack of effect (cAMP or pERK1/2 assays) in non-transfected cells is shown in Supporting Information (Figure S1).

■ ASSOCIATED CONTENT

Supporting Information

The Supporting Information is available free of charge on the ACS Publications website at DOI: 10.1021/acsomega.8b02509.

Lack of effect of piribedil and compounds **6** or **10** in cells that do not express dopamine receptors, that is, in untransfected HEK-293T cells (Figure S1) (PDF)

■ AUTHOR INFORMATION

Corresponding Authors

*E-mail: samadi@uaeu.ac.ae, samadi72@yahoo.com (A.S.).
*E-mail: h.saadeh@uaeu.ac.ae (H.A.S.).
*E-mail: iqoc21@iqog.csic.es (J.M.-C.).
*E-mail: rfranco123@gmail.com, rfranco@ub.edu. Phone: +34934021208 (R.F.)

ORCID

José Marco-Contelles: 0000-0003-0690-0328
Rafael Franco: 0000-0003-2549-4919

Author Contributions

▽I.R.-R., A.S., and G.N. have equally contributed to this work.

Notes

The authors declare no competing financial interest.

■ ACKNOWLEDGMENTS

R.F. appreciates the technical help provided by Jasmina Jiménez.

■ REFERENCES

(1) Hornykiewicz, O. The Discovery of Dopamine Deficiency in the Parkinsonian Brain. *Parkinson's Disease and Related Disorders*; Journal of Neural Transmission. Supplementa; Springer, 2006; Vol. *70*, pp 9−15.

(2) Dooley, M.; Markham, A. Pramipexole. *Drugs Aging* **1998**, *12*, 495−514.

(3) Mierau, J.; Schingnitz, G. Biochemical and Pharmacological Studies on Pramipexole, a Potent and Selective Dopamine D2 Receptor Agonist. *Eur. J. Pharmacol.* **1992**, *215*, 161−170.

(4) Molho, E. S.; Factor, S. A.; Weiner, W. J.; Sanchez-Ramos, J. R.; Singer, C.; Shulman, L.; Brown, D.; Sheldon, C. The Use of Pramipexole, a Novel Dopamine (DA) Agonist, in Advanced Parkinson's Disease. *J. Neural Transm., Suppl.* **1995**, *45*, 225−230.

(5) Zhou, W.; Zhong, G.; Fu, S.; Xie, H.; Chi, T.; Li, L.; Rao, X.; Zeng, S.; Xu, D.; Wang, H.; et al. Microglia-Based Phenotypic Screening Identifies a Novel Inhibitor of Neuroinflammation Effective in Alzheimer's Disease Models. *ACS Chem. Neurosci.* **2016**, *7*, 1499−1507.

(6) Mirzoeva, S.; Sawkar, A.; Zasadzki, M.; Guo, L.; Velentza, A. V.; Dunlap, V.; Bourguignon, J.-J.; Ramstrom, H.; Haiech, J.; Van Eldik, L. J.; et al. Discovery of a 3-Amino-6-Phenyl-Pyridazine Derivative as a New Synthetic Antineuroinflammatory Compound. *J. Med. Chem.* **2002**, *45*, 563−566.

(7) Hu, W.; Ralay Ranaivo, H.; Roy, S. M.; Behanna, H. A.; Wing, L. K.; Munoz, L.; Guo, L.; Van Eldik, L. J.; Watterson, D. M. Development of a Novel Therapeutic Suppressor of Brain Proinflammatory Cytokine Up-Regulation That Attenuates Synaptic Dysfunction and Behavioral Deficits. *Bioorg. Med. Chem. Lett.* **2007**, *17*, 414−418.

(8) Guo, X.; Nakamura, K.; Kohyama, K.; Harada, C.; Behanna, H. A.; Watterson, D. M.; Matsumoto, Y.; Harada, T. Inhibition of Glial Cell Activation Ameliorates the Severity of Experimental Autoimmune Encephalomyelitis. *Neurosci. Res.* **2007**, *59*, 457−466.

(9) Perez-Lloret, S.; Rascol, O. Piribedil for the Treatment of Motor and Non-Motor Symptoms of Parkinson Disease. *CNS Drugs* **2016**, *30*, 703−717.

(10) Gobert, A. Piribedil Enhances Frontocortical and Hippocampal Release of Acetylcholine in Freely Moving Rats by Blockade of Alpha 2A-Adrenoceptors: A Dialysis Comparison to Talipexole and Quinelorane in the Absence of Acetylcholinesterase Inhibitors. *J. Pharmacol. Exp. Ther.* **2003**, *305*, 338−346.

(11) Millan, M. J. From the Cell to the Clinic: A Comparative Review of the Partial D2/D3receptor Agonist and A2-Adrenoceptor Antagonist, Piribedil, in the Treatment of Parkinson's Disease. *Pharmacol. Ther.* **2010**, *128*, 229−273.

(12) Sweet, R. D.; Wasterlain, C. G.; McDowell, F. H. Piribedil, a Dopamine Agonist, in Parkinson's Disease. *Clin. Pharmacol. Ther.* **1974**, *16*, 1077−1082.

(13) Jenner, P.; Taylor, A. R.; Campbell, D. B. Preliminary Investigation of the Metabolism of Piribedil (ET 495); a New Central Dopaminergic Agonist and Potential Anti-Parkinson Agent. *J. Pharm. Pharmacol.* **1973**, *25*, 749−750.

(14) McLellan, D. L.; Chalmers, R. J.; Johnson, R. H. Clinical and Pharmacological Evaluation of the Effects of Piribedil in Patients with Parkinsonism. *Acta Neurol. Scand.* **1975**, *51*, 74−82.

(15) Jenner, P. An Overview of Adenosine A2A Receptor Antagonists in Parkinson's Disease. *Int. Rev. Neurobiol.* **2014**, *119*, 71−86.

(16) Elgueta, D.; Aymerich, M. S.; Contreras, F.; Montoya, A.; Celorrio, M.; Rojo-Bustamante, E.; Riquelme, E.; González, H.; Vásquez, M.; Franco, R.; et al. Pharmacologic Antagonism of Dopamine Receptor D3 Attenuates Neurodegeneration and Motor Impairment in a Mouse Model of Parkinson's Disease. *Neuropharmacology* **2017**, *113*, 110−123.

(17) Marcellino, D.; Ferré, S.; Casadó, V.; Cortés, A.; Le Foll, B.; Mazzola, C.; Drago, F.; Saur, O.; Stark, H.; Soriano, A.; et al. Identification of Dopamine D1-D3 Receptor Heteromers: Indications for a Role of Synergistic D1-D3 Receptor Interactions in the Striatum. *J. Biol. Chem.* **2008**, *283*, 26016−26025.

(18) Saadeh, H. A.; Khasawneh, M. A.; Samadi, A.; El-Haty, I. A.; Satała, G.; Bojarski, A. J.; Ismaili, L.; Bautista-Aguilera, Ó. M.; Yañez, M.; Mestres, J.; et al. Design, Synthesis and Biological Evaluation of Potent Antioxidant 1-(2,5-Dimethoxybenzyl)-4-Arylpiperazines and N-Azolyl Substituted 2-(4-Arylpiperazin-1-Yl). *ChemistrySelect* **2017**, *2*, 3854−3859.

(19) Saadeh, H. A.; Khasawneh, M. A.; Abu-Zeid, Y. A.; El-Haty, I. A.; Mubarak, M. S.; Nsangou, S. P.; Goyal, K.; Sehgal, R.; Marco-Contelles, J.; Samadi, A. Novel 5-Nitroimidazole and 5-Nitrothiazole Piperazine Derivatives and Their Antiparasitic Activity. *ChemistrySelect* **2017**, *2*, 5684−5687.

(20) Kaur, K.; Jain, M.; Reddy, R. P.; Jain, R. Quinolines and Structurally Related Heterocycles as Antimalarials. *Eur. J. Med. Chem.* **2010**, *45*, 3245−3264.

(21) Wang, Z.; Wang, Y.; Li, W.; Mao, F.; Sun, Y.; Huang, L.; Li, X. Design, Synthesis, and Evaluation of Multitarget-Directed Selenium-Containing Clioquinol Derivatives for the Treatment of Alzheimer's Disease. *ACS Chem. Neurosci.* **2014**, *5*, 952−962.

DOI: 10.1021/acsomega.8b02509
ACS Omega 2018, 3, 17368−17375

(22) El Faydy, M.; Dahaief, N.; Rbaa, M.; Ounine, K.; Lakhrissi, B. Synthesis, Characterization and Biological Activity of Some Novel 5-((4-Alkylpiperazin-1-Yl) Methyl) Quinolin-8-Ol Derivatives. *J. Mater. Environ. Sci.* **2016**, *7* (1), 356−361.
(23) Serrao, E.; Debnath, B.; Otake, H.; Kuang, Y.; Christ, F.; Debyser, Z.; Neamati, N. Fragment-Based Discovery of 8-Hydroxyquinoline Inhibitors of the HIV-1 Integrase-Lens Epithelium-Derived Growth Factor/P75 (IN-LEDGF/P75) Interaction. *J. Med. Chem.* **2013**, *56*, 2311−2322.
(24) Bautista-Aguilera, O. M.; Samadi, A.; Chioua, M.; Nikolic, K.; Filipic, S.; Agbaba, D.; Soriano, E.; de Andrés, L.; Rodríguez-Franco, M. I.; Alcaro, S.; et al. N-Methyl-N-((1-Methyl-5-(3-(1-(2-Methylbenzyl)Piperidin-4-Yl)Propoxy)-1H-Indol-2-Yl)Methyl)Prop-2-Yn-1-Amine, a New Cholinesterase and Monoamine Oxidase Dual Inhibitor. *J. Med. Chem.* **2014**, *57*, 10455−10463.
(25) Gaulton, A.; Hersey, A.; Nowotka, M.; Bento, A. P.; Chambers, J.; Mendez, D.; Mutowo, P.; Atkinson, F.; Bellis, L. J.; Cibrián-Uhalte, E.; et al. The ChEMBL Database in 2017. *Nucleic Acids Res.* **2016**, *45*, D945−D954.
(26) Van Eps, N.; Preininger, A. M.; Alexander, N.; Kaya, A. I.; Meier, S.; Meiler, J.; Hamm, H. E.; Hubbell, W. L. Interaction of a G Protein with an Activated Receptor Opens the Interdomain Interface in the Alpha Subunit. *Proc. Natl. Acad. Sci. U.S.A.* **2011**, *108*, 9420−9424.
(27) Chung, K. Y.; Rasmussen, S. G. F.; Liu, T.; Li, S.; DeVree, B. T.; Chae, P. S.; Calinski, D.; Kobilka, B. K.; Woods, V. L.; Sunahara, R. K. Conformational Changes in the G Protein Gs Induced by the B2 Adrenergic Receptor. *Nature* **2011**, *477*, 611−615.
(28) Dror, R. O.; Mildorf, T. J.; Hilger, D.; Manglik, A.; Borhani, D. W.; Arlow, D. H.; Philippsen, A.; Villanueva, N.; Yang, Z.; Lerch, M. T.; et al. Structural Basis for Nucleotide Exchange in Heterotrimeric G Proteins. *Science* **2015**, *348*, 1361−1365.
(29) Westfield, G. H.; Rasmussen, S. G. F.; Su, M.; Dutta, S.; DeVree, B. T.; Chung, K. Y.; Calinski, D.; Velez-Ruiz, G.; Oleskie, A. N.; Pardon, E.; et al. Structural Flexibility of the G s -Helical Domain in the 2-Adrenoceptor Gs Complex. *Proc. Natl. Acad. Sci. U.S.A.* **2011**, *108*, 16086−16091.
(30) Luginina, J.; Bizdēna, E.; Leonciks, A.; Kumpiņš, V.; Grīnšteine, I.; Turks, M. Synthesis and Antibacterial Activity of 5-Phthalate and 5-Glutarate Derivatives of Milbemycins A3/A4. *Chem. Heterocycl. Compd.* **2015**, *50*, 1404−1412.
(31) Medrano, M.; Aguinaga, D.; Reyes-Resina, I.; Canela, E. I.; Mallol, J.; Navarro, G.; Franco, R. Orexin A/Hypocretin Modulates Leptin Receptor-Mediated Signaling by Allosteric Modulations Mediated by the Ghrelin GHS-R1A Receptor in Hypothalamic Neurons. *Mol. Neurobiol.* **2018**, *55*, 4718−4730.
(32) Navarro, G.; Cordomí, A.; Brugarolas, M.; Moreno, E.; Aguinaga, D.; Pérez-Benito, L.; Ferre, S.; Cortés, A.; Casadó, V.; Mallol, J.; et al. Cross-Communication between Gi and Gs in a G-Protein-Coupled Receptor Heterotetramer Guided by a Receptor C-Terminal Domain. *BMC Biol.* **2018**, *16*, 24.
(33) Reyes-Resina, I.; Navarro, G.; Aguinaga, D.; Canela, E. I.; Schoeder, C. T.; Załuski, M.; Kieć-Kononowicz, K.; Saura, C. A.; Müller, C. E.; Franco, R. Molecular and Functional Interaction between GPR18 and Cannabinoid CB2G-Protein-Coupled Receptors. Relevance in Neurodegenerative Diseases. *Biochem. Pharmacol.* **2018**, *157*, 169−179.
(34) Navarro, G.; Varani, K.; Reyes-Resina, I.; Sánchez de Medina, V.; Rivas-Santisteban, R.; Sánchez-Carnerero Callado, C.; Vincenzi, F.; Casano, S.; Ferreiro-Vera, C.; Canela, E. I.; et al. Cannabigerol Action at Cannabinoid CB1 and CB2 Receptors and at CB1-CB2 Heteroreceptor Complexes. *Front. Pharmacol.* **2018**, *9*, 632.

DOI: 10.1021/acsomega.8b02509
ACS Omega 2018, 3, 17368−17375